

Effect of Cross-Linking on the Free-Volume Properties of Diethylene Glycol Bis(allyl carbonate) Polymer Networks: A Positron Annihilation Lifetime Study

G. Dlubek,^{*,†,‡} J. Stejny,[‡] and M. A. Alam[‡]

ITA Institut für Innovative Technologien GmbH, Köthen, Aussenstelle Halle, D-06124 Halle, Edvard-Grieg-Weg 8, Germany, and H. H. Wills Physics Laboratory, University of Bristol, Tyndall Avenue, Bristol BS8 1 TL, U.K.

Received December 10, 1997; Revised Manuscript Received April 22, 1998

ABSTRACT: The effect of cross-linking on the free-volume properties of poly(diethylene glycol bis(allyl carbonate)) networks was studied using a series of networks with progressively decreasing density of cross-links. The networks were prepared by bulk copolymerization of ethylene glycol bis(allyl carbonate) with an increasing amount of allyl ethoxyethyl carbonate. The mean free-volume hole radius (r) and the hole volume (v) as well as the hole radius and hole volume density distributions were estimated from positron lifetime measurements. It was found that with increasing concentration of monoallyl comonomer, the mean hole size increases from $r = 0.250$ nm ($v = 0.066$ nm³) for the pure diallyl component to 0.300 nm (0.114 nm³) for the 75% concentration of the monoallyl comonomer. Similarly, the hole size distributions shift to larger values. The local free-volume properties were correlated with the glass transition temperature and the specific volume. The comparison of the hole volume with the specific volume allowed us to estimate the number density of holes of $\sim 1 \times 10^{27}$ m⁻³ and a free-volume hole fraction which increases with the concentration of the monoallyl from 0.066 to 0.113.

Introduction

Recently, Stejny¹ has studied the relationship between the change in specific volume and cross-linking in the networks of the polymer poly(diethylene glycol bis(allyl carbonate)). He concludes that the observed change in the specific volume as a function of the degree of cross-linking in this system is dominated by a change in the free volume in these materials. In this paper, we investigate the free-volume properties of this polymer through positron annihilation lifetime (PAL) spectroscopy^{2–4} with a view to understanding the nature and distribution of local free volumes and its correlation with the degree of cross-linking. In recent years, PAL has been extensively utilized in the studies of free-volume characteristics in polymers.^{5–11} Here, we estimate the mean size and the size distribution of free-volume holes via analysis of positron lifetime spectra and discuss them in conjunction with previously published measurements of specific volumes (bulk density) and the glass transition temperatures on the same samples.¹

Experimental Section

The poly(diethylene glycol bis(allyl carbonate)) networks with a predetermined density of cross-links were prepared by bulk copolymerization of diethylene glycol bis(allyl carbonate), commonly known as CR-39 monomer, with different amounts of allyl ethoxyethyl carbonate as described by Stejny.¹ We investigated these copolymers in a range of composition containing a concentration fraction (c) between 0 and 75 wt % of the comonomer allyl ethoxyethyl carbonate, which gave a network with a corresponding T_g range from 112 °C to below room temperature.

The positron lifetime experiments were carried out at room temperature using a fast–fast coincidence system with a time

resolution of 235 ps (full width at half-maximum, fwhm, of a Gaussian resolution function) and a channel width of 12.5 ps. The specimens were platelets of 8×8 mm² in area and 1.5 mm in thickness. As a reference material, well-annealed aluminum platelets of similar dimensions were studied. For each experiment, two identical samples were sandwiched around a 5×10^6 Bq positron source (²²Na), prepared by evaporating carrier-free ²²NaCl solution on a capton foil of 8 μm thickness. Thirty-four measurements, each lasting 1200 s, were performed for each of the specimens and also for the reference materials. In a preliminary inspection, the time zero of each 1200-s spectrum was determined. The counts of those spectra where the time zero did not differ by more than one channel were summed to a final spectrum which contained a total number of $\sim 7 \times 10^6$ coincidence counts. There was no evidence of positron irradiation effects on the polymers under investigation in our experiments.

Results and Discussion

Analysis of the Positron Lifetime Spectra. While the lifetime of an individual positron may vary between 0 and ∞ , the lifetime spectrum of an ensemble of positrons annihilating from a solitary state is a single exponential $\exp(-t/\tau)$. τ denotes the mean lifetime of the positrons, which respond inversely to the electron density at the positron site. In molecular materials, such as polymers, a fraction of the injected positrons form and annihilate from a bound state called a positronium (Ps).^{2–4} The Ps appears either as a para positronium (p-Ps, singlet *spin* state) or as an ortho positronium (o-Ps, triplet *spin* state) with a relative abundance of 1:3. In a vacuum, an o-Ps has a relatively long lifetime of 142 ns. In matter, during collisions with molecules, the positron of the Ps may annihilate with an electron other than its bound partner and with opposite spin (pick-off annihilation). The result is a sharply reduced o-Ps lifetime depending on the frequency of collisions. In the presence of a sufficient concentration of small cavities in the sample, the Ps density is largely confined within these open volumes and their extent is reflected

[†] ITA Institut für Innovative Technologien.

[‡] University of Bristol.

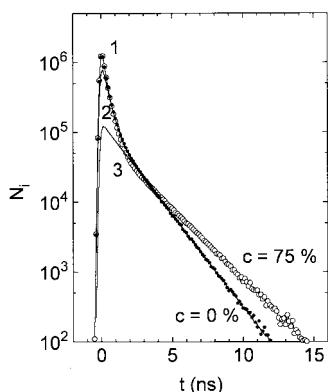


Figure 1. Positron lifetime spectra in pure poly(diethylene glycol bis(allyl carbonate)) and in the copolymer containing 75% monoallyl comonomer. Shown are the number of annihilation events (N_i) in channel i as a function of the time delay (t) between birth and annihilation of positrons. The experimental data are displayed after subtraction of the background and source components. For clarity, the content of five channels was added to get each data point. Each of the spectra consists of three components with lifetimes and intensities τ_i/I_i of 175 ps/23.1% (component 1), 406 ps/50.2% (component 2), 1640 ps/26.7% (component 3, $c = 0$ wt %), and 180 ps/23.0%, 410 ps/56.2%, and 2145 ps/20.7% ($c = 75$ wt %).

in the o-Ps pick-off lifetimes lying in the nanosecond-range. Typical positron lifetime spectra for amorphous polymers consist of three components. Two shorter ones arise from the annihilation of the p-Ps, of (free) positrons, and a long-lived component arises from the o-Ps annihilation.⁴⁻¹¹

As an example, the lifetime spectra of two samples with different degrees of cross-linking are plotted in Figure 1. It clearly demonstrates that, in addition to two shorter positron lifetimes, it contains a long-lived component. For a detailed analysis of the lifetime spectra, we used the conventional discrete-term analysis using the routine LIFSPECFIT¹² and the Laplace inversion program CONTIN-PALS2,¹³ which provides a continuous distribution of lifetimes in given intervals.

In the discrete-term model, the positron lifetime spectrum is assumed to be represented by a sum of negative exponentials,²⁻⁴

$$s(t) = \sum \lambda_i I_i \exp(-\lambda_i t) \quad (1)$$

where λ_i is the annihilation rate in the i th state with a relative intensity I_i ; $\sum I_i = 1$. The positron lifetime, which is usually under discussion, is the inverse of the annihilation rate, $\tau_i = 1/\lambda_i$. The analysis involves least-squares fitting of eq 1 following convolution with the experimental resolution. During the fitting, the usual correction procedure for positrons annihilating within the source and the containing materials is followed (380 ps/4%, NaCl and capton foil; 2500 ps/0.5%, surface effects). In keeping with visual indications in Figure 1, three lifetime components are resolved in the lifetime spectra arising from annihilation of p-Ps ($\tau_1 = 161$ –182 ps), free positrons ($\tau_2 = 390$ –415 ps), and a τ_3 in the nanosecond range due to o-Ps pick-off. Only the longest-lived component (τ_3) is sensitive to the physical and chemical structures within the specimen and shows a variation in the lifetime value and the component intensity with changing environment. In the copolymer containing between $c = 0$ and 75 wt % monoallyl comonomer, the o-Ps lifetime τ_3 increases from 1.640 to

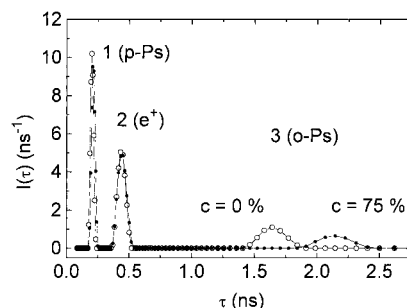


Figure 2. Positron lifetime intensity distribution $I(\tau)$ in pure poly(diethylene glycol bis(allyl carbonate)) (empty symbols) and in the copolymer containing 75 wt % monoallyl comonomer (filled symbols).

2.145(0.012) ns, while the relative intensity of this component, I_3 , decreases from 26.7% to 20.7% (0.2).

Instead of a sum of discrete exponentials, the CONTIN routine assumes a continuous decay form:¹³

$$s(t) = \int_0^\infty \lambda \alpha(\lambda) \exp(-\lambda t) d\lambda = L\{\lambda \alpha(\lambda)\} \quad (2)$$

Here, the annihilation decay integral is a Laplace transformation of $\lambda \alpha(\lambda)$. The fraction of positrons annihilating with rates between λ and $\lambda + d\lambda$ is $\alpha(\lambda) d\lambda$ and $\int \alpha(\lambda) d\lambda = 1$ (integration from 0 to ∞). The program CONTIN-PALS2¹³ allows the evaluation of the distribution function $\lambda \alpha(\lambda)$ from the experimental positron lifetime spectrum via a numerical Laplace inversion technique. The procedure also includes the deconvolution of the experimental resolution using a well-characterized reference spectrum. No assumption with respect to the shape of distribution $\alpha(\lambda)$ or to the width and shape of the resolution function has to be made.

The result of the CONTIN analysis of the two lifetime spectra of Figure 1 ($c = 0$ and 75 wt %) is plotted in Figure 2 in the form of the intensity distribution ($I(\tau)$) of the positron lifetimes. $I(\tau)$ relates to $\alpha(\lambda)$ via $I(\tau) = \lambda^2 \alpha(\lambda)$, $\lambda = 1/\tau$. During preliminary assessments, the intensity distribution was inspected over 90 grid points over the ranges of 0.01 to 33 ns and of 0.01 to 8 ns. No lifetime intensity below 0.1 ns and above 3 ns was observed. In the final analysis, the time interval was fixed at $0.08 < t < 3.33$ ns, within which the solutions of the numerical Laplace inversion were constrained to be positive. A second-order regularizer was employed to penalize deviations from smoothness. The result displayed in Figure 2 is the solution of eq 2 with a regularization parameter of 2.4×10^{-5} . Three well-separated peaks appear in the lifetime distribution which are related to the annihilation of p-Ps, free positrons, and o-Ps identified in the discrete-term analysis. The first moment and the relative area of the individual peaks agree within the error limits with the lifetime parameters τ_i and I_i obtained from the discrete-three-term analysis. Both Figures 1 and 2 clearly indicate that τ_1 and τ_2 remain almost unchanged, while τ_3 increases with increasing concentration of the monoallyl comonomer.

Mean Free-Volume Hole Size and Fractional Hole Volume. Due to the repulsive-exchange interaction between the electron in the Ps atom and the electrons of the molecules surrounding the positronium, Ps population tends to be confined in any available open spaces. It is a well-established view that in the amorphous phase in a polymer, the sites of Ps localization

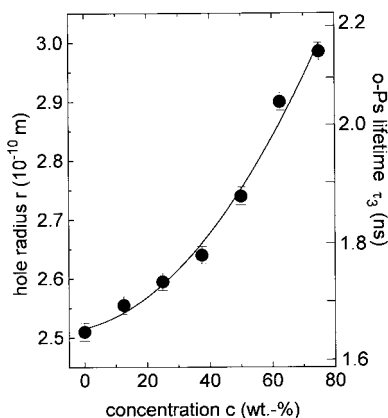


Figure 3. Dependence of the mean free-volume hole radius r (left axis) on the weight concentration c of the monoallyl comonomer. r was calculated by using eq 3 from the o-Ps lifetime τ_3 , which is indicated in the right axis of the figure.

are local holes of the free volume.^{4–11} A simple model incorporating quantum mechanical and empirical arguments provides an analytic expression relating the hole (assumed spherical) radius (r) to the observed o-Ps pick-off lifetime,^{6–9}

$$\tau_3 = \tau_{p0} = 0.5(\text{ns}) \left[1 - \frac{r}{r + \delta r} + \frac{1}{2\pi} \sin\left(\frac{2\pi r}{r + \delta r}\right) \right]^{-1} \quad (3)$$

The premultiplicative factor of 0.5 ns is the spin-averaged Ps annihilation lifetime which is also observed in densely packed molecular crystals.⁸ δr represents the extent of the penetration of the Ps wave function into the walls of the hole which is modeled by a square well potential of infinite depth and radius r . A widely used value of $\delta r = 0.166$ nm is obtained by fitting eq 3 to the observed o-Ps lifetime of the known mean hole radii in porous materials.^{7,9} Equation 3 allows the evaluation of either an average hole radius via a single τ_3 obtained from discrete-term analysis or, under the right conditions, a distribution of hole radii via a distribution of τ_3 given by the Laplace inversion technique.

In Figure 3, we present τ_3 (right-hand scale) for the copolymers as a function of the weight concentration of the monoallyl comonomer. Also displayed (in the left-hand scale) are the corresponding mean hole radii, calculated from τ_3 via eq 3. The τ_3 values were taken from the results of the discrete-three-term analysis of the lifetime spectra. These lifetimes have smaller statistical errors than those obtained by taking the first moment of the lifetime distributions of the longest component derived from the CONTIN analysis. This is due to the lowering of the degree of freedom in the fitting procedure by assuming a number of discrete lifetime terms.

The variation of τ_3 between 1.640 and 2.145(0.012) ns corresponds to a change in the mean hole radius from 0.250 to 0.300(0.0015) nm. The corresponding mean hole volume (v) varying between 0.066 and 0.113(0.001) nm³ is shown in Figure 4. Considering the structures of the polymers, the estimated mean free-volume hole size lies in a plausible range. The separation of neighboring carbon atoms in the hydrocarbons is 0.15 nm; bifunctional CH₂ and C₆H₄ groups occupy van der Waals volumes of 0.017 and 0.072 nm³, respectively.^{14,15} Mean hole sizes between 0.06 and 0.14 nm³ depending on the resin and curing conditions have been observed in various cross-linked epoxy resins.^{16–19} In glassy

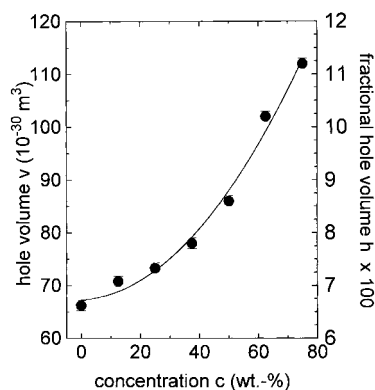


Figure 4. Dependence of the mean hole volume v (left axis) and of the fractional hole volume h (right axis) on the weight concentration c of the monoallyl comonomer. v was calculated from $v = 4r^3/3$ and h from $h = Nv$, where N is the number density of holes estimated to $\sim 1 \times 10^{27} \text{ m}^{-3}$ (see text).

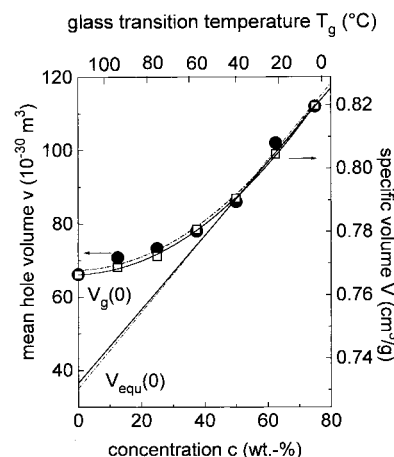


Figure 5. Dependence of the mean hole volume v (filled symbols, left axis) and of the macroscopic specific volume V (empty symbols, right axis) on the concentration c of the monoallyl comonomer. On the top axis, the glass transition temperature T_g is given which is related to c of the bottom axis via $T_g (\text{°C}) = 111 - 1.428c$ (wt %). (For the estimation of V and T_g as a function of c , see Stejny.¹)

polycarbonate and polystyrene, typical hole sizes of 0.1 nm³ are observed (see, for example, Dlubek et al.²⁰ and references given therein).

The plots in Figures 3 and 4 show that the free-volume hole size increases progressively from its minimum for the pure CR-39 to the value for the copolymer containing 75 wt % monoallyl comonomer. In a recent study, Stejny¹ found a gradual decrease in T_g from 112 °C in the pure CR-39 to 40 °C in the copolymer containing 50 wt % monoallyl comonomer. The increase in the hole size with increasing c is consistent with a decrease in T_g . Decreasing T_g indicates an increase in the specific volume and, therefore, larger hole volumes, which leads to the increase in τ_3 .

In Figure 5, we have plotted the dependence of v and of the specific volume (V) (taken from Stejny¹) on the concentration of the monoallyl comonomer. On the top axis, the T_g corresponding to c is also shown. Stejny obtained a good fit of the experimental points for the specific volume to a parabolic distribution $V (\text{cm}^3/\text{g}) = 9.105 \times 10^{-6}c^2 + 3.229 \times 10^{-5}c + 0.766$ (c given in wt %) with a correlation coefficient $\chi^2 = 0.99954$. It has to be noted that the density measurements were performed at 25 °C, which is below the glass transition temperature of all but two samples (see Figure 5). The struc-

tures of polymers are metastable below their glass transition temperatures. Thus, the values of the specific volume obtained below T_g are likely to be higher than those which correspond to the thermodynamic equilibrium. One may obtain the equilibrium specific volume by fitting a straight line to the data points of the samples which are in the rubbery phase (or sufficiently close to it) at the measuring temperature of 25 °C and extrapolating the line down to the glassy phase. Such a fit gives the equation $V_{eq} \text{ (cm}^3\text{/g)} = 1.17 \times 10^{-3}c + 0.732$. The difference between the measured specific volume and its equilibrium value increases with the difference between the T_g and the temperature of measurement.

We derive an equivalent expression for the equilibrium mean hole volume, $v_{eq}(10^{-30} \text{ m}^3) = 1.04c + 35$, by treating the mean hole volume data in the same fashion. The equilibrium hole volume for $c = 0\%$ (pure CR-39: lowest specific volume, closest packing), $v_{eq}(0) = 0.035 \text{ nm}^3$, corresponds to a hole radius of $r_{eq}(0) = 0.204 \text{ nm}$. According to eq 3, this hole size would correspond to an o-Ps lifetime of $\tau_3 = 1.25 \text{ ns}$. Lifetimes around this value appear often as an extra component in addition to a 2–4-ns o-Ps lifetime in semicrystalline polymers and are attributed to o-Ps annihilation in the crystalline phase.^{21,22} Since the crystalline phase may be considered as the most densely packed structure of the given polymer at a given temperature, we may interpret $2r_{eq}(0)$ to be closely related to the mean separation of molecular chains in the most densely packed structure (pure CR-39). The difference between the radius in the glassy phase, $r(0)$, and its extrapolated equilibrium value, $r_{eq}(0)$ (and corresponding $v(0)$ and $v_{eq}(0)$), reflects the increased separations of molecular chains on local sites and, in that way, the appearance of local free volumes in the metastable glassy phase of the polymer.

While plotting the hole and the specific volumes, v and V , versus the monoallyl monomer concentration in Figure 5, we have chosen the scales such that v and V coincide for the lower and upper boundary points, $c = 0\%$ and $c = 75\%$. It is interesting to observe that the variation in v correlates, within the error limits of the estimation, exactly with the behavior of V . For a semiquantitative discussion of this behavior, let us assume that the total specific volume is given by $V = V_0 + V_h = V_0 + N'v$. Here, V_0 is the total volume occupied by molecules, V_h is the free volume due to the holes, and N' and v denote the number of holes per gram and the mean hole volume. V_0 (which may also be called the bulk volume) consists of the van der Waals volume (V_W) and of an interstitial empty volume. V_h may be considered as an excess free volume appearing due to the disorder in the amorphous phase in addition to V_0 . If we assume that V_0 and N' are independent of the c of the monoallyl comonomer, we obtain the relation $(V(c) - V(0))/(V(75) - V(0)) = (v(c) - v(0))/(v(75) - v(0))$. The coincidence of the two curves in Figure 5 validates the derived relationship and therefore adds credence to the underlying assumptions that V_0 and N' are largely independent of c . That V_0 is independent of concentration in our case is a reasonable presumption. According to Bondi,¹⁴ V_0 may be approximated as $V_0 = 1.3 V_W$ at $T = 0 \text{ K}$. Since the CR39-monomer and the added comonomer are close in their chemical structures, V_W is likely to remain the same as a function of c . The assumption of constancy of N' throughout the concentration range may well be controversial. However, a fit

of the ratio $(V(c) - V(0))/(V(75) - V(0))$ assuming a linear increase of N' as a function of c indicates that the possible increase is less than 10%. We shall return to this point toward the end of this section.

In the following, we provide a more detailed discussion about the type of holes or local free volumes detected by the Ps probe and the possible ways of estimating the number of such holes and the fractional hole volume occupied by them. In amorphous polymers, an excess free volume appears due to the irregular molecular packing.^{23–25} This excess free volume may be considered to consist of irregularly shaped holes of varying size. The diffusion of gaseous or liquid molecules, for example, occurs across these holes.²⁶ Ps may be formed at any empty site in the sample. The thermalized Ps may migrate through the empty volume (the interstitial free volume) between the molecules and get trapped in a hole. Trapping occurs in a hole as the potential energy of the Ps inside a hole is lower than that outside due to the missing molecule which would repel the Ps. Finally, the Ps annihilates from a state inside a hole and its lifetime relates to the hole size according to eq 3. Following Simha and Boyer,²⁷ the fractional hole volume, denoted by h , may be defined as the relative volume in the amorphous phase being in excess to a hypothetical occupied volume $V_0 = V_{0,r}(1 + \alpha_g T)$, $h = (V - V_0)/V$, where V is the total volume. $V_{0,r}$ is the equilibrium volume of the amorphous polymer at 0 K. Assuming that the equilibrium volume at a given temperature behaves like $V_{eq} = V_{0,r}(1 + \alpha_r T)$, one may estimate $V_{0,r}$ by extrapolating linearly the temperature dependence of the total volume from the rubbery phase to 0 K. α_g and α_r denote the (cubic) coefficients of thermal expansion in the glassy and rubbery phases. From this, the following expression for the fractional hole volume at a given temperature can be derived:²⁷ $h = (V - V_{0,r}(1 + \alpha_g T))/V$. For $T = 0 \text{ K}$, we have

$$h(0) = (V_g(0) - V_{0,r})/V_g(0) = 1 - V_{0,r}/V_g(0) \quad (4)$$

Here, $V_g(0)$ is the total volume of the glassy polymer at $T = 0 \text{ K}$. h can be expected to increase slightly with the temperature in the range below T_g due to the anharmonicity of atomic oscillations. Above T_g , however, h will increase strongly due to the relaxation motion among the molecular chains. By applying this philosophy to our data, we may identify $V_g(0)$ with the specific volume of the pure CR-39 ($c = 0\%$) which is, at 25 °C, in a state well below the glass transition temperature of $T_g = 112 \text{ °C}$. We may obtain the volume representing $V_{0,r}$ by extrapolating the V versus c dependence from the rubbery phase ($c > 50\%$) linearly to the intercept with the vertical axis at $c = 0\%$ (see Figure 5). The experimental value of the specific volume is $0.766 \text{ cm}^3\text{/g}$ for $c = 0\%$; the extrapolated equilibrium volume amounts to $0.732 \text{ cm}^3\text{/g}$. From these values, we estimate a fractional hole volume $h = 0.0448$ at $c = 0\%$.

As the next step, we estimate the number of holes per m^3 , N , from h and v for $c = 0\%$ using the relation

$$h = Nv \quad (5)$$

This yields a value of $N = h/v = 0.0448/0.066 \text{ nm}^3 = (0.68 \pm 0.2) \times 10^{27} \text{ m}^{-3}$. Using a relation analogous to eq 4, a number density of holes of $0.4 \times 10^{27} \text{ m}^{-3}$ has been recently estimated for glassy polycarbonate from thermal expansion experiments.²⁶ Positron annihilation studies²² during thermal expansion in the amorphous

phases of PE and PTFE have yielded N values of 0.73×10^{27} and $0.36 \times 10^{27} \text{ m}^{-3}$. Thus, our value for the number of holes per unit volume falls within a narrow range observed for different polymers. It has to be noted, however, that the ratio $V_{0,r}/V_g(0)$ in eq 4 is only approximated by the ratio $V_{eq}(0)/V(0)$, which does not correspond to a true extrapolation of V_r and V_g to absolute zero temperature. Since $\alpha_r > \alpha_g$,^{15,27} the values of h and N estimated from the data in Figure 5 may be considered as lower limits of the true values.

For a further confirmation of the conclusion that the number density of holes in our samples is largely unaffected by the concentration of the comonomer, we use another approach to estimate N . Again we assume that the change in the specific volume, $V(c)$, with increasing c of the monoallyl comonomer is controlled exclusively by the change in the total hole volume, $V(c) = V_h(c) + V_o(0)$. The total hole volume per gram is given by $V_h(c) = N'(c) \nu(c)$, where N' and ν denote, as previously, the number of holes per gram and the mean hole volume. For $c = 0$, we have $V_h(0) = N'(0) \nu(0)$ and $V_o(0) = V(0) - N'(0) \nu(0)$. With $V_o(c) = V_o(0)$,

$$V(c) = N'(c) \nu(c) + [V(0) - N'(0) \nu(0)] \quad (6)$$

follows. To take into account a possible variation of N' with c , we assume that $N'(c)$ changes as

$$N' = N'(0)(1 + Ac) \quad (7)$$

Equations 6 and 7 may be now fitted to the experimental points using $N'(0)$ and A as the fitting parameters. From a least-squares fitting procedure we got $N'(0) = (1 \pm 0.2) \times 10^{21} \text{ g}^{-1}$ (corresponding to $(1.3 \pm 0.3) \times 10^{27} \text{ m}^{-3}$) and $A = 0.1 \pm 0.1$. These results, although based on a different approach, are in sufficient agreement with our previous number of $N(0) = 0.68 \times 10^{27} \text{ m}^{-3}$, which we have considered as a lower limit of the true $N(0)$. By using $N'(0) = 1 \times 10^{21} \text{ g}^{-1}$, $\nu(0) = 0.066 \text{ nm}^3$, and $V(0) = 0.766 \text{ cm}^3/\text{g}$, we find $V_o(c=0) = V(0) - N'(0) \nu(0) = 0.700 \pm 0.013 \text{ cm}^3/\text{g}$, a value very close to that estimated for the pure CR-39 from Bondis approximation $V_o(T=0 \text{ K}) = 1.3V_w = 0.682 \text{ cm}^3/\text{g}$. Due to the thermal expansion of the interstitial free volume ($0.3V_w$ at $T = 0 \text{ K}$), V_o expands with increasing temperature approximately like the glassy polymer, $V_o = V_{o,r}(1 + \alpha_g T)$.^{15,27} Since $V_o(300 \text{ K}) > V_o(0 \text{ K}) \approx V_o(c=0)$, the above estimation of $N = (1.3 \pm 0.3) \times 10^{27} \text{ m}^{-3}$ may be considered as an upper limit of the true number density of holes. When we take into consideration the estimated upper and lower limits, $N = (1.0 \pm 0.4) \times 10^{27} \text{ holes/m}^3$ may be accepted as a realistic value.

As shown in Figure 6, the o-Ps intensity I_3 decreases from 26.7% to 20.7% when the concentration of the comonomer increases from 0 to 75%. In the literature,^{9,17,30,32} I_3 is often interpreted as a measure of the number of holes per unit volume, viz. $N(c) = CI_3(c)$ and $h(c) = CI_3(c) \nu(c)$, where C is assumed to be a constant. Between $c = 0\%$ and $c = 75\%$, the value of I_3 decreases by a factor of 0.775, while, accepting our previous approximations (6) and (7), N is constant within a range of $\pm 10\%$. This discrepancy may be understood as follows. I_3 is a measure of the Ps yield (P), $I_3 = 3P/4$, assuming no Ps quenching channels others than pick-off annihilation. The Ps yield may be controlled by various factors, such as electron and positron mobilities and the presence of "scavengers", for example.⁴ The number of holes is only one of these factors. Evidently,

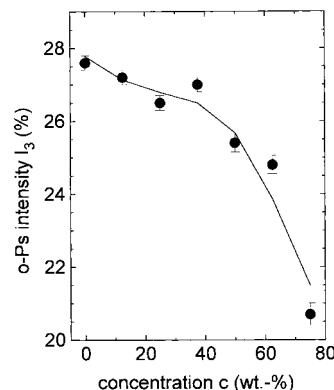


Figure 6. Dependence of the o-Ps intensity I_3 on the weight concentration c of the monoallyl comonomer.

the Ps yield decreases in our samples with increasing concentration of comonomer due to reasons yet to be ascertained. It has been observed, for example, that in PE (PTFE) the o-Ps intensity increases in the temperature range between 80 and 200 K (150 K) but decreases after that range due reasons which cannot be attributed to a corresponding variation in the number of free-volume holes.²²

The fractional hole volume as sampled by the Ps probe, h , may then be estimated from eq 5 using a constant $N = 1 \times 10^{27} \text{ m}^{-3}$ and the mean hole volume given in Figure 4. The values obtained in this manner are indicated in the right-hand scale of Figure 4. The fractional hole volume changes, of course, in a fashion similar to ν , from 0.066 for $c = 0\%$ to 0.113 for $c = 75\%$. Our estimates of the fractional hole volume at $T = T_g = 25^\circ \text{C}$, $h(60\%) = 0.093$, are significantly larger than the often accepted value²⁸ of $h(T_g) = 0.025$. We note, however, that the value of 0.025 is estimated from viscosity experiments via the WLF theory.^{28,29} Such a procedure may only involve larger local free volumes needed for the transportation of larger molecular segments and a significant fraction of the free volume may not contribute to the viscosity. For amorphous polymers such as polystyrene, polycarbonate, poly(vinyl acetate), and poly(methyl methacrylate), $h(T_g)$ values of 0.06–0.09 have been estimated from a combination of positron lifetime and thermal expansion experiments.^{17,30–34} Using a similar approach, $h(T_g)$ values of 0.045 and 0.057 were estimated for the amorphous phases of polyethylene and poly(tetrafluoroethylene) ($T_g = 195 \text{ K}$).²²

Hole Size Probability Density Function. Having discussed various aspects of the average hole within our samples, we now turn to aspects of the possible size distributions of the holes. As stated earlier, the continuous lifetime analysis of positron annihilation spectra in amorphous polymers here and by others provides three well-separated peaks of finite widths (Figure 2). If the unique correspondence of the o-Ps lifetime and the free-volume hole radius given by eq 3 are assumed to be valid, the lifetime distribution may be transformed into a hole radii distribution. An expression for the probability density function (pdf) of the hole radii $f(r)$ is derived as $\alpha(\lambda) d\lambda/dr$

$$f(r) = -3.32\{\cos[2\pi r/(r + \delta r)] - 1\} \alpha(\lambda)/(r + \delta r)^2 \quad (8)$$

where r is the radius of an individual local hole of the free volume, $\lambda = 1/\tau$, and $r = 0.166 \text{ nm}$.^{35,36} The fraction of o-Ps annihilation in the holes with radii between r

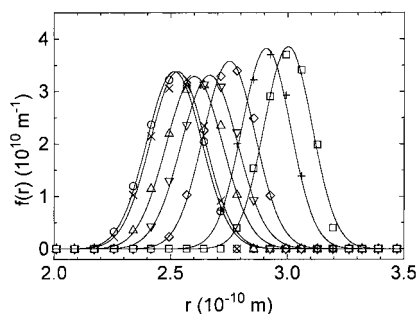


Figure 7. Hole radius probability distribution function $f(r)$ as a function of the weight concentration c of the monoallyl comonomer. The distributions which were calculated according to eq 8 from the o-Ps lifetime distributions shift to higher values with increasing c (wt %) = 0, 12.5, 25, 37.5, 50, 62.5, and 75. The distributions are normalized so that $\int f(r) dr = 1$. The smooth curves represent single Gaussians least-squares-fitted to each of the distributions.

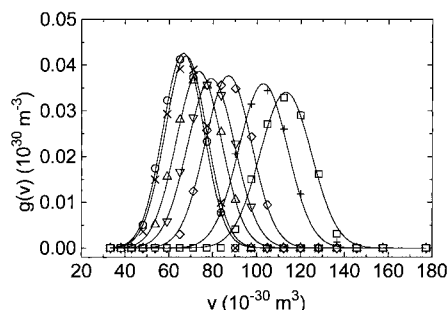


Figure 8. Hole volume probability distribution function $g(v)$ as a function of the weight concentration c of the monoallyl comonomer. The distributions were calculated according to eq 9 from the data shown in Figure 7. The distributions are normalized so that $\int g(v) dv = 1$. The smooth curves represent single Gaussians least-squares-fitted to each of the distributions.

and $r + dr$ is $f(r) dr$. The hole radius pdf given by eq 6 may be converted into a hole volume probability density distribution via

$$g(v) = f(r)/4r^2 \quad (9)$$

The volume fraction of holes as determined by o-Ps annihilation in holes with volume between v and $v + dv$ is $g(v) dv$. By multiplying eq 9 with an appropriately chosen constant, the probability density function may be normalized so that $\int g(v) dv = 1$ or h (integration from 0 to ∞ , where h denotes the total volume fraction of the free-volume holes in the specimen).

The hole radius and the hole volume pdf's $f(r)$ and $g(v)$ estimated via eqs 8 and 9 are plotted in Figures 7 and 8 for the copolymers with different concentrations of monoallyl comonomer. The distributions were normalized such that $\int g(v) dv = 1$. We observe a gradual shift of the hole size distributions to larger values with increasing c . In each case, the first moment of the hole size distributions agrees well with the mean hole radius and volume estimated from the discrete τ_3 values discussed in the previous section (Figures 3 and 4). The hole radius probability density functions presented in Figure 6 appear to be perfectly symmetric and are well approximated by Gaussians centered between 0.249 and 0.299 nm and a fwhm around 0.028 nm. The hole volume pdf for each sample can also be fitted with sufficient accuracy by a Gaussian with centers between 0.0665 and 0.113 nm³ and a fwhm around 0.025 nm³.

This type of distribution has been predicted by the free-volume theory of Bueche³⁷ and has also been observed in other glassy polymers such as polycarbonate and polystyrene.²⁰

Conclusion

The mean size of the free-volume holes in poly(diethylene glycol bis(allyl carbonate)) networks prepared by bulk copolymerization of ethylene glycol bis(allyl carbonate) with an increasing amount of allyl ethoxyethyl carbonate increases with increasing concentration of the monoallyl comonomer from $r = 0.250$ nm ($v = 0.066$ nm³, $c = 0\%$) to 0.300 nm (0.113 nm³, $c = 75\%$).

The relative change of the mean hole volume agrees exactly with the relative change of the specific volume. From this, it is concluded that the number of holes does not change as a function of c .

From a comparison of v and V , a number density of holes of $(1.0 \pm 0.4) \times 10^{27}$ m⁻³, i.e., 1 hole/nm³, and a free-volume hole fraction increasing with c from 0.066 to 0.113, $h_g = h(60\%) = 0.093$, were estimated. The o-Ps intensity was found to decrease from 26.7% to 20.7% when the concentration of the comonomer increases from 0 to 75%. This behavior was attributed to a decreasing Ps yield.

The hole radius and the hole volume distributions shift with increasing concentration to larger values, in good correlation with the mean hole size.

Acknowledgment. This work was carried out with the support of the Commission of the European Community through the program "LEONARDO DA VINCI". G.D. thanks the University of Bristol for the support as visiting scientist. P. Hautojärvi (Helsinki) and Y. C. Jean (Kansas City) are acknowledged for supplying the PC versions of the routines LIFSPECFIT and CONTIN-PALS2.

References and Notes

- (1) Stejny, J. *Polymer Bull.* **1996**, *36*, 617.
- (2) Hautojärvi, P., Ed. *Positrons in Solids; Topics in Current Physics*; Springer-Verlag: Berlin, 1979; Vol. 12.
- (3) Brandt, W.; Dupasquier, A., Eds. *Positron Solid-State Physics; Proc. Int. School of Physics "Enrico Fermi"*, Varenna 1981; North-Holland: Amsterdam, 1983.
- (4) Mogensen, O. E. *Positron Annihilation in Chemistry*; Springer-Verlag: Berlin, Heidelberg, 1995.
- (5) Brandt, W.; Berko, S.; Walker, W. W. *Phys. Rev.* **1960**, *15*, 1289. Brandt, W.; Fahs, J. H. *Phys. Rev. B* **1970**, *17*, 1425.
- (6) Tao, S. J. *J. Chem. Phys.* **1972**, *56*, 5499.
- (7) Eldrup, M.; Lightbody, D.; Sherwood, J. N. *Chem. Phys.* **1981**, *63*, 51.
- (8) Lightbody, D.; Sherwood, J. N.; Eldrup, M. *Chem. Phys.* **1985**, *93*, 475.
- (9) Nakahishi, N.; Jean, J. C. In *Positron and Positronium Chemistry, studies in physical and theoretical chemistry*, 57; Schrader, D. M., Jean, Y. C., Eds.; Elsevier: Amsterdam, 1988; p. 159. Jean, Y. C. In *Positron Annihilation, Proc. of the 10th Int. Conf.*; He, Y.-J., Cao, B.-S., Jean, J. C., Eds.; Mater. Sci. Forum 175–178; Trans Technol.: 1995; p. 59.
- (10) *Proceedings of the 5th Int. Workshop on Positron and Positronium Chemistry*, June 9–14, 1996; Kajcsos, Zs., Levay, B., Süvegh, K., Eds.; ppc5. Lillafüred, Hungary. *J. Radioanal. Nucl. Chem.* **1996**, *210* (2), 255–642; **1996**, *211* (1), 1–282.
- (11) Pethrick, R. A. *Prog. Polym. Sci.* **1997**, *22*, 1.
- (12) LIFSPECFIT 5.1. *Lifetime spectrum fit version 5.1*; Technical University of Helsinki, Laboratory of Physics: 1992.
- (13) CONTIN-Version 2DP. Provencher, S. W. *Comput. Phys. Commun.* **1982**, *27*, 213. *EMBL Technical Report DA 05*; European Molecular Biology Laboratory: Heidelberg, 1982. Gregory, R. B.; Zhu, Y. *Nucl. Instrum. Meth. A* **1990**, *290*, 172. Gregory, R. B. *Nucl. Instrum. Meth. A* **1991**, *302*, 496.

- (14) Bondi, A. *J. Phys. Chem.* **1964**, *68*, 441. *Physical Properties of Molecular Crystals, Liquids, and Gases*; Wiley: New York, 1968; p 450.
- (15) Van Krevelen, D. W. *Properties of Polymers*; Elsevier: Amsterdam, 1990.
- (16) Jean, Y. C.; Sandreczki, T. C.; Ames, D. P. *J. Polym. Sci.: Polym. Phys.* **1986**, *24*, 1247.
- (17) Wang, Y. Y.; Nakanishi, H.; Jean, Y. C. *J. Polym. Sci., Part B: Polym. Phys.* **1990**, *28*, 1431.
- (18) Jeffrey, K.; Pethrick, R. A. *Eur. Polym. J.* **1994**, *30*, 153.
- (19) Venditti, R. A.; Gillham, J. K.; Jean, Y. C.; Lou, J. *J. Appl. Polym. Sci.* **1995**, *56*, 1207.
- (20) Dlubek, G.; Clarke, A. P.; Fretwell, H. M.; Dugdale, S. B.; Alam, M. A. *Phys. Stat. Sol. (A)* **1996**, *157*, 351.
- (21) Serna, J.; Abbe, J. Ch.; Duplatre, G. *Phys. Stat. Sol. (A)* **1989**, *115*, 389.
- (22) Dlubek, G.; Saarinen, K.; Fretwell, H. M. *J. Polym. Sci.: Part B: Polym. Phys.* **1998**, *36*, 1513. Dlubek, G.; Saarinen, K.; Fretwell, H. M. *Nucl. Instrum. Meth. B* **1998**, *142*, 139.
- (23) Simha, R.; Somcynsky, T. *Macromolecules* **1969**, *2*, 342.
- (24) Goldstein, M.; Simha, R. *The Glass Transition and the Nature of the Glassy State*; New York Academy of Science: New York, 1976.
- (25) Allen, G.; Petrie, S. E. B., Eds. *Physical Structure of the Amorphous State*; Marcel Dekker: New York, 1976.
- (26) Jordan, S. S.; Koros, W. J. *Macromolecules* **1995**, *28*, 2228.
- (27) Simha, R.; Boyer, R. F. *J. Chem. Phys.* **1962**, *37*, 1003.
- (28) Williams, M. L.; Landel, R. F.; Ferry, J. D. *J. Am. Chem. Soc.* **1955**, *77*, 3701.
- (29) Doolittle, A. K. *J. Appl. Phys.* **1951**, *22*, 1471.
- (30) Kobayashi, Y.; Zheng, W.; Meyer, E. F.; McGervey, J. D.; Jamieson, A. M.; Simha, R. *Macromolecules* **1989**, *22*, 2, 2303.
- (31) Kluin, J.-E.; Yu, Z.; Vleeshouwers, S.; McGervey, J. D.; Jamieson, A. M.; Simha, R. *Macromolecules* **1992**, *25*, 5089.
- (32) Yu, Z.; Yashi, U.; McGervey, J. D.; Jamieson, A. M.; Simha, R. *J. Polym. Sci.: Part B: Polym. Phys.* **1994**, *23*, 2637.
- (33) Xie, L.; Gidley, D. W.; Hristov, H. A.; Yee, A. F. *J. Polym. Sci.: Part B: Polym. Phys.* **1995**, *33*, 77.
- (34) Hristov, H. A.; Bolan, B.; Ye, A. F.; Xie, L.; Gidley, D. W. *Macromolecules* **1996**, *29*, 8507.
- (35) Deng, Q.; Jean, Y. C. *Macromolecules* **1993**, *26*, 30.
- (36) Liu, J.; Deng, Q.; Jean, Y. C. *Macromolecules* **1993**, *26*, 7149.
- (37) Bueche, F. *J. Chem. Phys.* **1953**, *21*, 1850.

MA971801Y